Suppressors of the Arabidopsis *lsd5* Cell Death Mutation Identify Genes Involved in Regulating Disease Resistance Responses

Jean-Benoit Morel[1] and Jeffery L. Dangl

Department of Biology and Curriculum in Genetics and Molecular Biology, University of North Carolina, Chapel Hill, North Carolina 27599-3280

Manuscript received July 13, 1998
Accepted for publication September 15, 1998

ABSTRACT

Cell death is associated with the development of the plant disease resistance hypersensitive reaction (HR). Arabidopsis *lsd* mutants that spontaneously exhibit cell death reminiscent of the HR were identified previously. To study further the regulatory context in which cell death acts during disease resistance, one of these mutants, *lsd5*, was used to isolate new mutations that suppress its cell death phenotype. Using a simple lethal screen, nine *lsd5* cell death suppressors, designated *phx* (for the mythological bird *Ph*oeni*x* that rises from its ashes), were isolated. These mutants were characterized with respect to their response to a bacterial pathogen and oomycete parasite. The strongest suppressors—*phx2*, *3*, *6*, and *11-1*—showed complex, differential patterns of disease resistance modifications. These suppressors attenuated disease resistance to avirulent isolates of the biotrophic *Peronospora parasitica* pathogen, but only *phx2* and *phx3* altered disease resistance to avirulent strains of *Pseudomonas syringae* pv *tomato*. Therefore, some of these *phx* mutants define common regulators of cell death and disease resistance. In addition, *phx2* and *phx3* exhibited enhanced disease susceptibility to different virulent pathogens, confirming probable links between the disease resistance and susceptibility pathways.

PLANTS are constantly challenged by infectious pathogens. However, because plants have developed sophisticated defense mechanisms, disease rarely occurs. One correlate of disease resistance, called the hypersensitive response (HR; Agrios 1988; Goodman and Novacky 1994), is manifested by the local triggering of a set of defense reactions and cell death. This localized plant cell death, around the infection site, may be responsible for halting pathogen growth. Alternatively, HR could be a cellular consequence of the mechanism that actually stops pathogen growth. HR is often governed by single genes in both the plant (resistance or *R*-gene) and the pathogen (avirulence or *avr* gene). Disease resistance is observed only when matching *R* and *avr* specificities are present (gene-for-gene relationship; Flor 1947).

The HR pathway can be separated into three steps: *R*-gene-mediated recognition of the pathogen, transduction of signals to the nucleus, and execution of the defense program. The cloning of several *R*-genes has led to the observation that, despite the diversity of pathogens recognized by these genes, common structural features are found among the proteins they encode (Bent 1996). Subsequent to recognition, signal transduction pathways are engaged. A number of different signals have been implicated in the triggering of the HR (Hammond-Kosack and Jones 1996). Generation of reactive oxygen intermediates (the oxidative burst; Baker and Orlandi 1995) and changes in ion fluxes (Atkinson and Baker 1989) are observed during the early phases of many plant-pathogen interactions. Finally, defense genes such as the PR (pathogenesis-related; Linthorst 1991) are activated and defense products such as phytoalexins (Smith 1996) can be synthesized.

It is unclear what contributions cell death and defense gene activation make in halting pathogen growth. Cell death may be the result of the induction of defense products, many of which are toxic for the plant cell. However, HR cell death seems to be intrinsically controlled by the plant. Several lines of evidence support the idea that HR cell death is a form of programmed cell death (Mittler and Lam 1996; Morel and Dangl 1997). The best evidence derives from the existence of mutants, called lesion mimics, that spontaneously exhibit cell death reminiscent of the HR in the absence of pathogen. Such mutants have been found in maize (Walbot *et al.* 1983), barley (Wolter *et al.* 1993), and other species (Dangl *et al.* 1996). In Arabidopsis, *acd* (Greenberg and Ausubel 1993; Greenberg *et al.* 1994) and *lsd* mutants (lesion simulating disease resistance; Dietrich *et al.* 1994) have been identified. In addition to the spontaneous cell death phenotype, these mutants exhibit hallmarks of the plant defense response, such as expression of defense genes and ectopic disease resistance.

Corresponding author: Jeffery L. Dangl, Department of Biology, University of North Carolina, CB#3280, Coker Hall 108, Chapel Hill, NC 27599-3280. E-mail: dangl@email.unc.edu

[1] *Present address:* Laboratoire de Biologie Cellulaire, INRA Versailles, 78026 Cedex, France.

On the basis of their phenotypes, two classes of *lsd* mutations were established. In the first class, lesions do not spread once initiated (initiation class). Most lesion mimic mutations that belong to this class (*e.g.*, *lsd5*; Dietrich *et al.* 1994). It was hypothesized that these mutations represent defects in genes involved in the triggering of the HR cell death pathway (Dangl *et al.* 1996; Mittler and Lam 1996). In the second class of mutations (propagation class), lesions spread once they have been initiated (*e.g.*, *lsd1*; Dietrich *et al.* 1994). These mutations define genes necessary for the control of the extent of cell death (Dietrich *et al.* 1997). Recently, several of the genes responsible for cell death phenotypes have been cloned. The *LSD1* gene encodes a novel class of zinc finger protein that could act as a negative regulator of signals involved in the propagation of cell death (Dietrich *et al.* 1997). The *LLS1* gene from maize encodes a putative dioxygenase that could be responsible for the detoxification of signals generated during cell death (Gray *et al.* 1997). Finally, the *MLO* resistance gene from barley encodes a putative transmembrane protein (Büschges *et al.* 1997). The cloning of such genes and the study of their regulation will help define the regulatory components of cell death in plants.

Different approaches have been used to analyze genetically HR cell death. In the first, the phenotype used to define mutants consisted of loss of disease resistance to a particular avirulent pathogen. This led to the identification of loci *r*equired for *d*isease *r*esistance (*RDR* loci; Hammond-Kosack and Jones 1996), such as *ndr1* (Century *et al.* 1995) and *eds1* (Parker *et al.* 1996). Both of these mutations identify Arabidopsis genes required for resistance to multiple pathogens and triggered by multiple *R*-genes. Identification of these mutations suggests a possible convergence of the pathways triggered by distinct *R*-genes. Interestingly, both these mutants also exhibited enhanced growth of normally virulent pathogens, suggesting that the pathways leading to resistance and susceptibility share some components.

In other studies, Glazebrook and Ausubel (1994) and Glazebrook *et al.* (1997) directly addressed the role of one component of the defense response: They looked for mutants affected in the biosynthesis of the major Arabidopsis antimicrobial phytoalexin, camalexin. All *pad* mutants were impaired in resistance to virulent isolates of the oomycete *Peronospora parasitica*. However, those mutations had little impact on restricting growth of an avirulent strain of *Pseudomonas syringae*. Interestingly, those mutants are still able to mount an HR (Glazebrook and Ausubel 1994), suggesting that camalexin cannot be directly reponsible for cell death.

Using a similar approach, we aimed at elucidating the role of the HR in the disease resistance pathway. We isolated suppressor mutations of the Arabidopsis *lsd5* cell death control mutant. Some of these exhibited reduced resistance to avirulent pathogens and define new loci that modify disease resistance mechanisms. The results presented here support a model in which the genetic components regulating cell death are also required in plant disease resistance.

MATERIALS AND METHODS

***lsd5* seeds mutagenesis and suppressors screening:** Seeds of the *lsd5* mutant (accession Ws-0; Dietrich *et al.* 1994) were mutagenized with either fast-neutrons (0.031 Gy/s) or ethyl methanesulfonate (EMS 0.15% for 8 hr). M_1 plants (600 and 100 for the fast neutron and EMS mutagenesis, respectively) were grown under permissive conditions for *lsd5* [16-hr light; long day (LD)] in 20 pools of 1 to 20 plants for each mutagenesis. Approximately 40 M_2 seeds per M_1 plant were then sown under nonpermissive conditions [8-hr light; short day (SD), 60 μEinsteins total fluence] for suppressor screening. *In vitro* cultivation of *lsd5* and M_3 seeds from M_2 candidate plants was performed on Murashige and Skoog medium (Gibco BRL, Gaithersburg, MD) solidified with 0.8% agar and supplemented with 50 μg/ml kanamycin to select for a T-DNA linked to *lsd5* (J.-B. Morel and J. Dangl, unpublished results).

Bacteria and Peronospora growth conditions: *P. syringae* pv *tomato* DC3000 (*Pst* DC3000; Whalen *et al.* 1991) and *P. syringae* pv *glycinea R4* (*Psg*; Kobayashi *et al.* 1989) were cultured overnight in modified King's B medium (20 g/liter peptone, 20 g/liter tryptone, 20 g/liter glycerol, 0.05% K_2HPO_4, 0.05% KH_2PO_4) supplemented with 100 μg/ml rifampicin. Kanamycin (30 μg/ml) was added in cultures of *Pst* DC3000 and *Psg* containing the avirulence gene *avrRpm1* (Debener *et al.* 1991) or *avrRps4* (Hinsch and Staskawicz 1996) cloned into the pVSP61 vector (Bisgrove *et al.* 1994) and in cultures of *Psg* containing the empty vector pVSP61. Spores of *P. parasitica* isolates Ahco2, Noco2, and Emwa1 were prepared via propagation (Dangl *et al.* 1992), using the susceptible ecotypes Col-0 and Ws-0, respectively. An *rpp5* mutant (*rpp5* P41; Parker *et al.* 1997) was used to ensure identity of the isolates Noco2 and Ahco2.

Bacterial growth and HR assays: Four-wk-old plants grown under short days were hand inoculated on half leaves with *Pst* DC3000 strains at a dose of 10^5 cfu/ml in 10 mm $MgCl_2$ (OD_{600} = 0.0002), using a syringe (with no needle). At various time points, samples (consisting of four leaf disks of ~0.28 cm^2, each from separate infected plants) were ground in 10 mm $MgCl_2$ and 10-fold serial dilutions plated on modified King's B medium (1.5% agar) containing the appropriate antibiotics and cycloheximide (50 μg/ml, to prevent growth of other microbes). Data are reported as means and standard deviations of the log (cfu/cm^2). For HR tests with *Psg* strains, solutions containing 3×10^8 cfu/ml (OD_{600} = 0.6) were hand inoculated on a small leaf area. In both assays, humidity was kept high for 24 hr by covering the plants.

Peronospora infection assay: Freshly prepared spore suspensions (40 spores/μl in water) were sprayed to runoff on 10- to 14-day-old seedlings using a sprayer (Preval, New York). To include *lsd5* in these experiments, plants were grown under long-day and shifted to short-day conditions (8-hr light, 16°, 100% humidity) after inoculation to ensure appropriate Peronospora growth conditions. Samples were analyzed 1 day and 5 days after inoculation using trypan blue staining. In each independent experiment, from 25 to 150 interaction sites (5–30 cotyledons, ~5 interaction sites per cotyledon) were scored for each time point and for each genotype. For sporulation analysis with *P. parasitica* isolate Emwa1, 20 cotyledons were harvested, weighed, and washed in 100–200 μl water

(vortexed twice 15 sec). Spores were then counted using a hemocytometer (magnification ×100).

Trypan blue staining: Plant tissue was heated 3 min at 95° in trypan blue solution (Koch and Slusarenko 1990) and left to stain overnight. After destaining in chloral hydrate (2.5 g dissolved in 1 ml of water) for 2 days, samples were mounted in 70% glycerol for microscopy analysis.

Statistical analysis: For segregation analysis, the χ^2 test was used (1 d.f.). For pathology experiments, Student's *t*-test was used to compare the means of the different mutant lines and Ws-0.

Allelism tests and double mutant isolation: Allelism between the *phx/lsd5* mutants and the *ndr1-1* (Col-0; Century *et al.* 1995), *pad4-1* (Col-0; Glazebrook *et al.* 1997), and *eds1-1* (Ws-0; Parker *et al.* 1996) was assayed as follows: The recessive *phx/lsd5* mutants were crossed to the different mutants. Allelism in F_1 plants was determined using the loss-of-resistance phenotypes associated with *P. parasitica* isolate Ahco2 for *eds1-1* and isolate Emwa1 for *pad4-1* and *ndr1-1*. The strain *Pst* DC3000 carrying the avirulence gene *avrRpt2* (Whalen *et al.* 1991) was also used to test allelism to *ndr1-1*. For double mutant isolation, *lsd5* was crossed to the *eds1-1* and *ndr1-1* mutants. Lesioned plants (homozygous for *lsd5*) were selected in the F_2 progeny and the genotype for the *eds1-1* or the *ndr1-1* mutation was then determined using a PCR marker specific for the *eds1-1* mutation (J. Parker, personal communication). Preselection for the *ndr1-1* mutation among lesioned F_2 plants (homozygous for *lsd5*) was performed by PCR using CAPS marker GAPA, which is linked to this locus. Confirmation of the presence of the *ndr1-1* mutation, which results in the absence of *NDR1* mRNA (Century *et al.* 1997), was obtained by RNA blot analysis in the selected F_3 families.

Separation of the *phx* mutations from the *lsd5* mutation: The *lsd5* mutation is tightly linked to a 1.3-kb truncated T-DNA, as well as to a functional kanamycin resistance gene (see results). Segregation analysis showed that the genetic distance between the 1.3-kb T-DNA and the *lsd5* phenotype was <0.36 cM. However, the *lsd5* mutant is not tagged (J.-B. Morel and J. L. Dangl, unpublished results). We designed primers from the flanking genomic sequences of this T-DNA. Because both wild-type and *lsd5* alleles could be amplified by PCR, this codominant marker (called TOC) was used to genotype plants at *lsd5*. Lesion minus F_2 plants from crosses between Ws-0 and the different *phx/lsd5* mutants (backcrossed once; see results) that were heterozygous for the TOC marker were selfed. Segregation of kanamycin resistance was also tested in the F_3 progeny to further confirm heterozygosity at the *lsd5* locus. Finally, segregation of the *lsd5* phenotype was examined in each resulting F_3 population under SD. When no *lsd5* plant was found in an F_3 family, we inferred that the *phx* mutation was originally homozygous in the parent F_2 plant. Because the *lsd5* mutation was presumably segregating in such an F_3 family, individual F_3 plants were analyzed with the TOC PCR, and plants where no *lsd5* PCR allele was detected were considered homozygous *phx* and wild type at the *LSD5* locus. Confirmation of the genotype was obtained by crossing the isolated *phx* lines to *lsd5* and Ws-0. Thus, isolated *phx* lines are the product of two backcrosses.

DNA extraction, PCR conditions, and mapping techniques: Small-scale genomic DNA preps were made from ~0.25 cm^2 leaf disks ground in 400-μl extraction buffer (200 mm Tris-HCl, pH 7.5, 250 mm NaCl, 25 mm EDTA, 0.5% SDS). Samples were centrifuged 3 min at 13,000 rpm, the supernatant was precipitated with 300 μl isopropanol, and the pelleted DNA was resuspended in 20 μl TE. DNA (1 μl) was used in a 20-μl PCR reaction. For the TOC PCR, conditions were 94° 3 min, 40× (94° 30 sec, 50° 1 min, 72° 3 min), 72° 5 min. TOC *lsd5*-specific primers were 5′-CCAGTCAAAGGAAGAAAGAGA-3′ (TIC2) and 5′-ATGCGTGGTTCAATGTTTTAT-3′ (TAC2). Mapping was done using PCR-based CAPS (Konieczny and Ausubel 1993) and simple sequence length polymorphisms (Bell and Ecker 1994) markers. Other markers were obtained from the Arabidopsis database (http://genome-www.stanford.edu/Arabidopsis/).

RNA blot analysis: Total RNA was purified using 1 ml of TRIZOL reagent (Gibco BRL) per ~0.5 ml of tissue ground in liquid nitrogen according to the manufacturer's protocol. Samples (5 μg/lane) were separated on formaldehyde-agarose gels (Ausubel *et al.* 1995), transferred to Hybond-N hybridization membrane (Amersham, Buckinghamshire, UK), hybridized in HYBSOL solution (Yang *et al.* 1993), and washed 30 min in 2× SSC, 0.1% SDS at 65° and 30 min in 1× SSC, 0.1% SDS at 50°. Radiolabeled probes were generated using the random oligolabeling kit from Stratagene (La Jolla, CA). The probes used were cDNAs for *PR1* (Uknes *et al.* 1992) and 18S rRNA (kindly provided by E. Lam, Rutgers, NJ).

RESULTS

Isolation of *lsd5* suppressors by conditional lethal screening: As described in Dietrich *et al.* (1994), the recessive *lsd5* mutation is conditional. Grown under long days (16-hr light, LD), *lsd5* plants are smaller than wild type (Ws-0) and rarely develop spontaneous foliar lesions. However, when transferred from long-day to short-day conditions (8-hr light, SD), adult *lsd5* plants show macroscopic lesions 3–4 days later. More importantly, when grown under constant SD, the *lsd5* mutation is lethal. We took advantage of this conditional lethality to isolate second site mutations that suppress *lsd5*. Mutagenized *lsd5* M_2 seeds (fast neutron and EMS) were sown under SD, and plants that survived under these conditions were further analyzed. The *lsd5* mutation is tightly linked to a kanamycin resistance gene (<0.39 cM; J.-B. Morel and J. L. Dangl, unpublished results) originating from the T-DNA used to obtain this mutant line (Dietrich *et al.* 1994). M_3 seeds from the putative mutants were analyzed for their resistance to kanamycin, and only mutants that were homozygous for this *lsd5*-linked marker were selected. M_3 progeny were sown under SD to confirm the suppressed phenotype. In some cases, M_4 progeny from individual M_3's had to be tested to obtain homozygous suppressor mutations that had been isolated as M_2 heterozygote individuals. On the basis of these criteria, a total of 11 mutants, all from independent M_1 lots, were isolated (Figure 1): 4 after fast neutron mutagenesis (0.6 = *phx1*, 4.2 = *phx2*, 8.12 = *phx3*, and 18.2 = *phx4*) and 7 after EMS mutagenesis (2.3 = *phx9*, 3.6 = *phx10*, 6.1 = *phx11-1*, 10.26 = *phx12*, 14.1 = *phx11-2*, 16.1 = *phx8*, and 17.10 = *phx6*; see below).

Two phenotypic classes were readily distinguishable (Figure 1). Some mutants were fully suppressed for the presence of lesions, and the remaining mutants developed some lesions late in development but did not exhibit the early developmental lethality of the *lsd5* phenotype. This classification was confirmed by examination of microscopic cell death in leaf tissues from plants

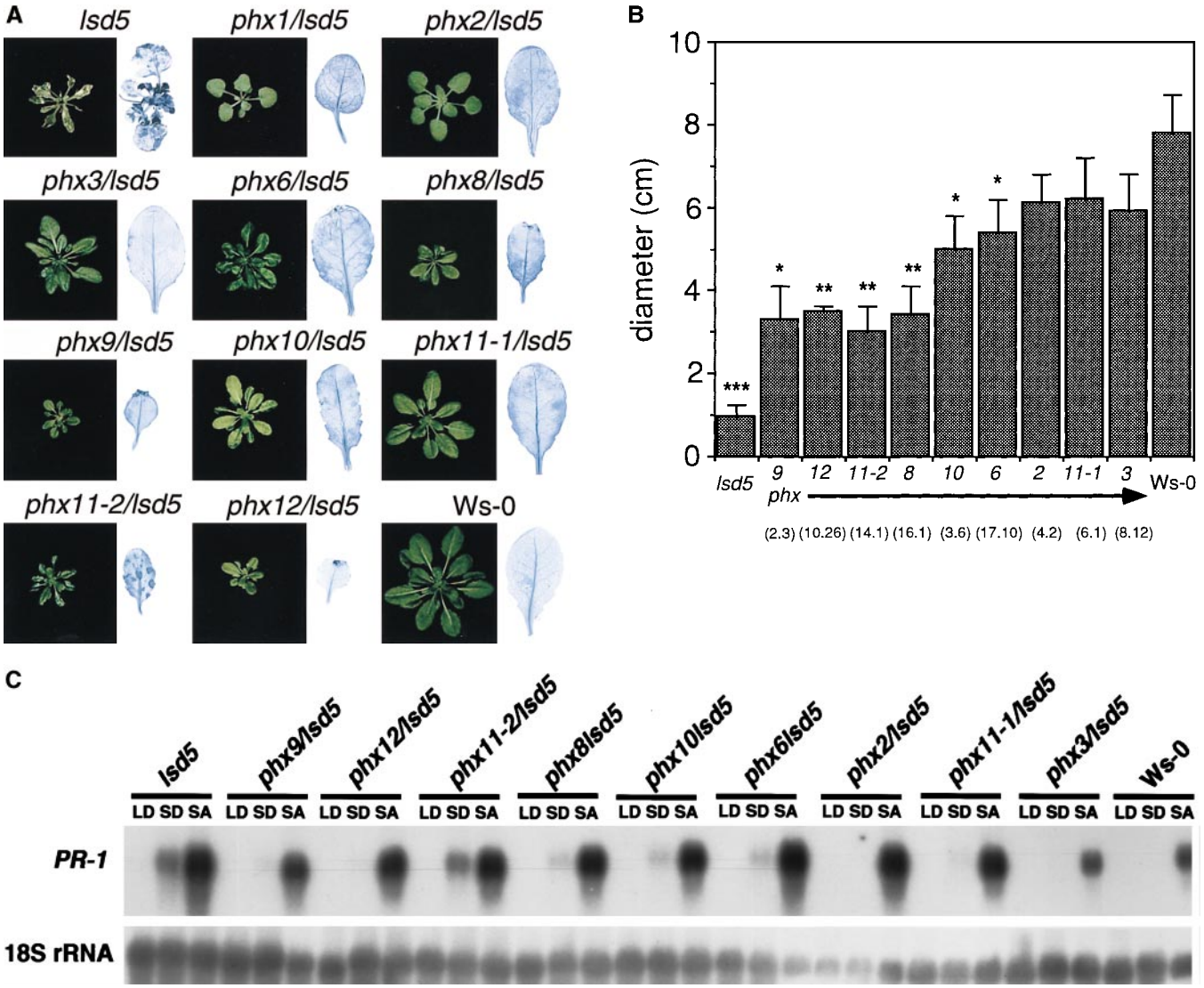

Figure 1.—Reversion of the *lsd5* cell death phenotype in the *phx*/*lsd5* mutants. Each suppressor line and controls (wild type Ws-0 and *lsd5*) were grown under SD for 4 wk. (A) Macroscopic phenotypes. A plant is displayed for each line (left) and one typical leaf after staining for cell death with trypan blue (right). *lsd5* pictures are magnified four times compared to the others. (B) Size measurements of the original *phx*/*lsd5* lines (the numbers in parentheses refer to the original mutant designation; see Tables 1 and 2). Mean and standard deviation of the largest diameter of 12 plants. The percentage of plants exhibiting macroscopic lesions is indicated: *, 25%; **, 75%; and ***, 100%. (C) Reversion of the *lsd5 PR1* gene expression phenotype. Three-week-old plants grown under long days (LD) were shifted to short days for induction of *lsd5* lesions and RNA was extracted after 7 days (SD) or treated (under LD) with SA (0.5 mg/ml) and RNA extracted 2 days after treatment (SA). RNA samples (5 μg/lane) were hybridized with a *PR1* probe and, after stripping, with an 18-S rRNA probe as a loading control. Experiments were repeated at least two times and gave similar results.

grown under SD (using trypan blue staining as a marker of cell death; see Figure 1A). Rosette size measurements also reflected the degree of *lsd5* suppression (Figure 1B). The lines 4.2, 6.1, and 8.12, which are fully suppressed for lesion formation, reached ~75% of the size of wild-type plants, while the other lines were significantly smaller (Figure 1B). In addition to the macroscopic and microscopic examination of the suppression phenotypes, we assessed defense gene expression in the double mutants (Figure 1C). Constitutive *PR1* expression has been shown to be associated with the HR-like *lsd5* lesions under SD (Dietrich *et al.* 1994). *PR1* is not inducible in the strong suppressor lines after shifting plants from LD to SD, as observed in *lsd5*, although the weak suppressor lines exhibited low levels of induction (Figure 1C). Consistent with the suppression of *lsd5* lesions in plants continuously grown under SD, *PR1* mRNA was undetectable in most of the suppressor lines, with the exception of several weak suppressors (lines 2.3, 14.1, 16.1, and 17.10; not shown). We also addressed whether *PR-1* was still inducible in those lines by application of salicylic acid (SA), a natural inducer of systemic

TABLE 1

Genetic analysis of *lsd5* suppressors

Cross[a]	F_1[b]		F_2[c] segregation				
	Lsd5$^-$	Lsd5$^+$	Lsd5$^-$	Lsd5$^+$	Ratio[d]	n.h.	χ^2, P[d]
0.6 × *lsd5*	0	5	7	57	1:8.1	1:3	6.75, <0.01r
Ws-0 × 0.6	33	0	212	51	4.1:1	13:3	0.07, >0.09
4.2 × *lsd5*	25	0	249	74	3.4:1	3:1	0.75, >0.5
Ws-0 × 4.2[e]	9	0	3076	0	1:0	1:0	0
8.12 × *lsd5*	47	0	67	11	6.1:1	3:1	4.94, <0.02r
Ws-0 × 8.12	28	0	355	15	23.7:1	15:1	2.47, >0.2
18.2 × *lsd5*	0	3	4	14	1:3.5	1:3	0.07, >0.9
Ws-0 × 18.2	3	0	485	157	3.1:1	3:1	0.10, >0.9
2.3 × *lsd5*	0	2	18	68	3.8:1	1:3	0.76, >0.5
Ws-0 × 2.3	8	0	96	26	3.7:1	13:3	0.53, >0.5
3.6 × *lsd5*	0	11	27	56	1:2.1	1:3	0.76, >0.5
Ws-0 × 3.6	5	0	88	17	5.2:1	13:3	0.45, >0.5
6.1 × *lsd5*	0	9	11	42	1:3.8	1:3	0.51, >0.5
Ws-0 × 6.1	5	0	459	0	1:0	1:0	0
10.26 × *lsd5*	0	12	42	124	1:3	1:3	0.01, >0.9
Ws-0 × 10.26	23	0	98	17	5.8:1	13:3	1.19, >0.3
14.1 × *lsd5*	0	8	31	80	1:2.6	1:3	0.51, >0.5
Ws-0 × 14.1	2	0	71	0	1:0	1:0	0
16.1 × *lsd5*	0	5	66	225	3.4:1	3:1	0.84, >0.5
Ws-0 × 16.1	5	0	43	3	14.3:1	13:3	4.52, <0.02r
17.10 × *lsd5*	0	3	8	14	1:1.8	1:3	1.51, >0.3
Ws-0 × 17.10	2	0	47	14	3.4:1	13:3	2.3, >0.2

[a] Crosses are listed female × male. All F_2s with Ws-0 were segregating *lsd5* genotype as assayed by segregation of resistance to kanamycin (not shown).
[b] Plants were grown under LD and shifted to SD after 3 wk to induce *lsd5* lesions.
[c] Tests performed under SD.
[d] Segregation data was evaluated with chi-square analysis using the null hypothesis (n.h.) indicated. Chi-square probabilities are indicated. Rejection of the null hypothesis is indicated (r).
[e] Crosses were done in both directions and gave similar results.

acquired resistance (SAR) and defense-related genes (Ward *et al.* 1991). As shown in Figure 1C, *PR-1* mRNA accumulation was inducible by SA under LD in all the suppressors to levels comparable to *lsd5*. Similar results were obtained for SA induction of *PR1* in plants grown continuously under SD (not shown).

Genetic analysis of the *lsd5* suppressor mutants: Because suppression of the *lsd5* phenotype could result from reversion of the initial recessive *lsd5* mutation, both intragenic and extragenic suppressors were expected. F_1 and F_2 analyses of backcrosses to *lsd5* and crosses to Ws-0 were used to establish inheritance of the *phx* mutations. The following types of *phx* mutations were found (Table 1): recessive and linked to *lsd5* (6.1, 14.1, and 16.1), dominant and linked (4.2), recessive and extragenic (0.6, 2.3, 3.6, 10.26, 17.10, and 18.2), and dominant extragenic (8.12). While F_1 and F_2 data from the cross 16.1 × *lsd5* shows that the 16.1 locus is recessive, an unexpected ratio of ~15 wild type:1 *lsd5* was found in F_2 from the cross Ws-0 × 16.1 (instead of the 13 wild type:3 *lsd5* ratio expected if 16.1 is recessive and unlinked). This can be explained by genetic linkage between the *lsd5* and 16.1 loci. In contrast, we were unable to separate, out of more than 3000 meioses, the suppressor mutation in the line 4.2 from the *lsd5* mutation. It is likely that this suppressor corresponds to an intragenic mutation (distance to *lsd5* <0.017 cM). Similarly, the 6.1 and 14.1 mutations are tightly linked to the *lsd5* mutation and may represent intragenic revertants. Because the 4.2 mutant was dominant, allelism between this mutation and the recessive 6.1 and 14.1 mutations could not be addressed. Despite unexpected segregation ratios observed in the F_2 of the cross 8.12 × *lsd5*, further analysis and genetic separation of the suppressor mutation from *lsd5* confirmed that the mutation in the line 8.12 is extragenic and dominant (see below).

Complementation testing was used to determine how many loci were defined by the eight extragenic recessive suppressors (0.6, 2.3, 3.6, 6.1, 10.26, 14.1, 16.1, and 17.10). *phx*/*lsd5* double mutants were crossed pairwise, and the resulting F_1 seeds sown under SD. The mutations in lines 6.1 and 14.1 failed to complement (Table 2) and therefore represent allelic mutations. It is noteworthy that the 6.1 line is a significantly stronger allele than 14.1 (see Figure 1). All other intercrosses still expressed the *lsd5* early lethal phenotype in SD, indicat-

TABLE 2

Complementation testing of *lsd5* extragenic recessive suppressors lines

Pollen *phx* recipient	Designation	Pollen donor 0.6	2.3	3.6	6.1	10.26	14.1	16.1	17.10
0.6	*phx1*		+	+	+	+	+	+	+
2.3	*phx9*	+		+	+	*	+	+	*
3.6	*phx10*	*	*		+	+	*	*	*
6.1	*phx11-1*	*	*	*		+	−	+	+
10.26	*phx12*	+	+	*	*		+	+	+
14.1	*phx11-2*	*	*	+	−	*		+	+
16.1	*phx8*	*	*	+	*	*	+		+
17.10	*phx6*	*	+	+	*	*	*	*	

For each cross, more than five F_1 seeds were tested for *lsd5* phenotype under SD.
(*) Not tested but reciprocal cross tested.
(+) Complementation; (−) no complementation.

ing that these mutants represent mutations in different genes (Table 2). Based on this genetic analysis, at least seven complementation groups were obtained. These mutants were named *phx* after the mythological *Ph*oeni*x* that rises from its ashes as follows: *phx1*/*lsd5* (0.6), *phx2*/*lsd5* (4.2), *phx3*/*lsd5* (8.12), *phx6*/*lsd5* (17.10), *phx8*/*lsd5* (16.1), *phx9*/*lsd5* (2.3), *phx10*/*lsd5* (3.6), *phx11-1*/*lsd5* (6.1), *phx11-2*/*lsd5* (14.1), and *phx12*/*lsd5* (10.26). Due to its instability after backcross to *lsd5*, mutant 18.2 (*phx4*/*lsd5*) was not further analyzed. Similarly, *phx5* is lethal in combination with *lsd5*. *phx1* will be described elsewhere. All experiments described below were using progeny of lines backcrossed to *lsd5* and reselected as not segregating for phenotypic suppression of *lsd5* lesions.

Bacterial resistance in the double *phx*/*lsd5* mutants: As a preliminary test that the *lsd5* suppressors may impair disease resistance, we monitored the growth of the normally avirulent *Pst* DC3000 (*avrRpm1*) bacteria in the *phx*/*lsd5* mutants. The presence of the *RPM1* resistance gene in wild-type Ws-0 plants (the background for *lsd5*) treduces up to 1000-fold the growth of bacteria carrying the *avrRpm1* avirulence gene as compared to the isogenic strain lacking *avrRpm1* (Grant *et al.* 1995; Figure 2). As shown in Figure 2A, two suppressor lines, *phx2*/*lsd5* and *phx3*/*lsd5*, showed a significant loss of resistance to this normally avirulent isolate 1 day postinoculation (dpi). No significant differences between the other suppressor lines and Ws-0 were detected in these experiments 1 dpi (Figure 2A) or 3 dpi (not shown). The *phx2*/*lsd5* and *phx3*/*lsd5* mutants were therefore further characterized. As shown in Figure 2B, 1 dpi, both suppressor lines allowed bacterial multiplication similar to that observed during the compatible interaction between Ws-0 and *Pst* DC3000. Bacterial titers remained slightly higher in the *phx2*/*lsd5* and *phx3*/*lsd5* than in Ws-0 at later time points. In addition, chlorotic symptoms associated with the compatible interaction between Ws-0 and *Pst* DC3000 were visible in these two lines by 5 dpi (Figure 3). It is noteworthy that under these light conditions *lsd5* plants normally show enhanced levels of resistance to pathogens (Dietrich *et al.* 1994) and that despite the presence of the *lsd5* mutation, the *phx2*/*lsd5* and *phx3*/*lsd5* mutants displayed reduced resistance. Plants heterozygous for either *phx2* or *phx3* also exhibited disease-like symptoms, suggesting that this phenotype, like the *lsd5* suppression phenotype, is dominant (Figure 3A).

We also tested whether resistance triggered by a different combination of *R-avr* genes was modified in the *phx*/*lsd5* lines. Plants were inoculated with the normally avirulent *Pst* DC3000 (*avrRps4*) (Hinsch and Staskawicz 1996) and bacterial growth measured. We did not measure any significant difference in bacterial growth or changes in symptoms between the *phx*/*lsd5* lines and Ws-0 (1 and 3 dpi; data not shown).

Reaction to the oomycete *P. parasitica* in the *phx*/*lsd5* mutants: *lsd5* plants exhibit enhanced resistance to the virulent *P. parasitica* isolate Emwa1 (Dietrich *et al.* 1994). We wanted to measure the possible effects of the suppressor mutations on this phenotype under conditions where *lsd5* exhibits little or no cell death. Plants were therefore grown under LD and shifted to SD after inoculation with different *P. parasitica* isolates (SD; high humidity conditions are required for optimal Peronospora growth). Under these conditions, almost no spontaneous cell death was visible in *lsd5* until day 3 after shift to SD, although background cell death could be measured microscopically (data not shown).

Interactions involving biotrophic oomycetes such as *P. parasitica* differ significantly from interactions between plants and necrotrophic bacteria. In particular, plant cell death may play a different role in interactions involving necrotrophic and biotrophic pathogens (Morel and Dangl 1997). The use of this pathosystem also allows for detailed characterization of the cellular events during infection of cotyledons (Koch and Slusarenko 1990; Holub *et al.* 1994; Holub and Beynon 1997). We

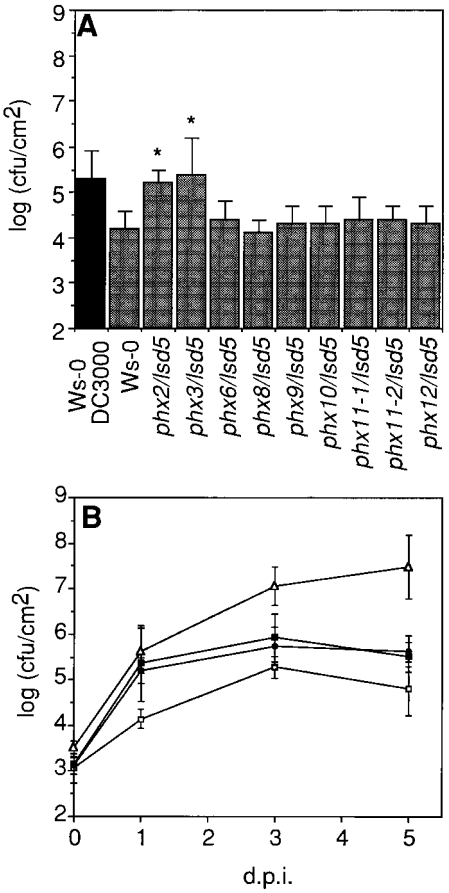

Figure 2.—Modification of disease resistance to *P. syringae* in the *phx*/*lsd5* mutants. Plants grown under SD were hand-inoculated with 10^5 cfu/ml of *Pst* DC3000 (+/− *avrRpm1*). At the indicated times, samples were cut from infected leaves and bacterial titers were determined. (A) *Pst* DC3000 (*avrRpm1*) 1 day postinoculation (dpi) in the *phx*/*lsd5* mutants and Ws-0 (gray bars). *Pst* DC3000 in Ws-0 (black bar) was also included as a growth-positive control. Stars indicate a statistically significant difference between Ws-0 and the corresponding lines ($P > 99\%$) using a Student's *t*-test. (B) Open triangles, *Pst* DC3000 in Ws-0; open squares, *Pst* DC3000 (*avrRpm1*) in Ws-0; solid circles, *Pst* DC3000 (*avrRpm1*) in *phx2*/*lsd5*; solid squares, *Pst* DC3000 (*avrRpm1*) in *phx3*/*lsd5*. The *t* values and confidence limits 1 dpi for *Pst* DC3000 (*avrRpm1*) are as follows: Ws-0-*phx2*/*lsd5*, 5.36 (>99%); Ws-0-*phx3*/*lsd5*, 2.53 (>95%). Each point represents the mean and standard deviation of four to five independent experiments. Because these experiments were done under SD, *lsd5* could not be included.

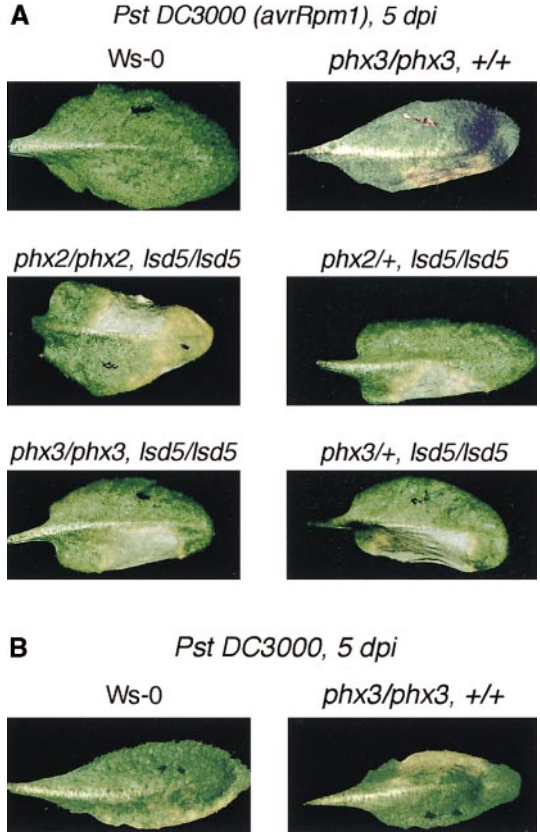

Figure 3.—Disease symptoms in the *phx2* and *phx3* mutants. (A) Plants were hand-inoculated with 10^5 cfu/ml of *Pst* DC3000 (*avrRpm1*) and pictures taken 5 dpi. Wild-type Ws-0 is symptomless (resistant), while all the other lines exhibit extensive chlorosis. F_1 plants heterozygous for the *phx2* and *phx3* loci express symptoms similar to homozygous lines. Photos are representative of 25 leaves per genotype, and the experiment was repeated four times. (B) Plants were inoculated with 10^5 cfu/ml of *Pst* DC3000 and disease symptoms pictured 5 dpi. Photos are representative of 15 leaves per genotype from one experiment.

used trypan blue staining to detect both fungal structures and plant cells showing either increased membrane permeability (light blue staining) or collapse (dark staining and absence of recognizable cell shape). Typically, six major types of reaction sites were observed during an incompatible interaction (Figure 4). After adhesion to the plant leaf surface, the spore had germinated and given rise to an infection structure called a haustorium (Figure 4A). From this point, two sets of events occurred. One was characterized by reaction of the infected plant cells (haustorium with reaction, Figure 4B) and later development of a typical HR (Figure 4C), as described by Koch and Slusarenko (1990), with intact neighboring mesophyl cells exhibiting light staining with trypan blue. In the other series of events, which only accounts for ~20% of the incompatible interaction sites in Ws-0 for either of the two isolates used, there was no apparent plant cell reaction and the parasite grew further (free hyphae, Figure 4D). The plant cells eventually detected those hyphae, leading to light trypan blue staining (hyphae with reaction, Figure 4E). Finally, HR occurred but behind hyphal growth, as suggested by the presence in some cases of hyphae emerging from HR (hyphae in HR, Figure 4F).

As a first characterization of the *phx*/*lsd5* lines, we measured the frequency of HR (as in Figure 4C) after challenge with the avirulent isolates Ahco2 (recognized by an *R* gene near *RPP12*; Holub and Beynon 1997) and Noco2 (recognized in Ws-0 by the *RPP1/10/14* complex; Reignault *et al.* 1996; Botella *et al.* 1998). For

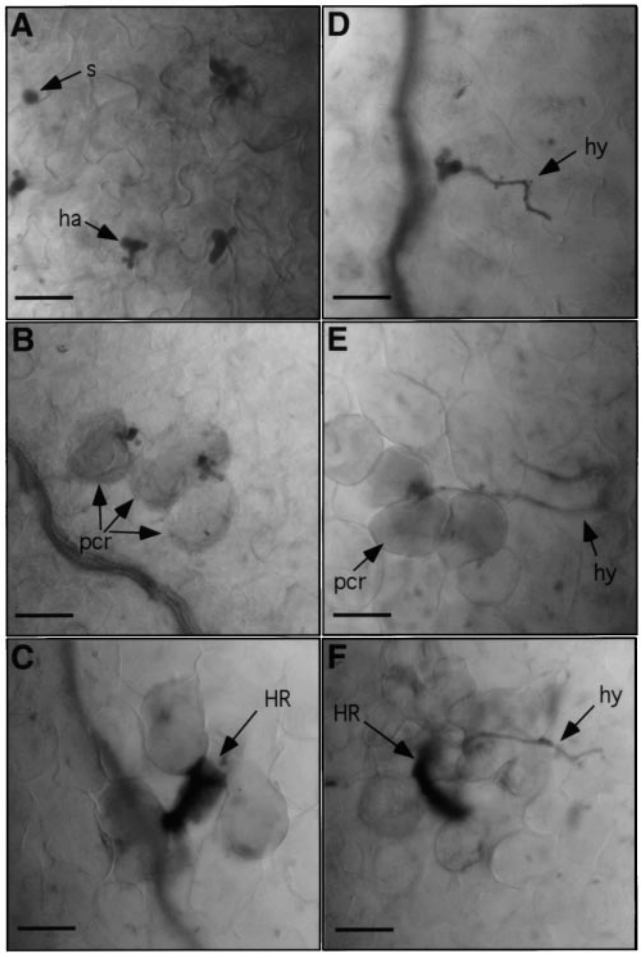

Figure 4.—Cellular interaction between Ws-0 and incompatible isolates of *P. parasitica*. Two-week-old seedlings were sprayed with a spore suspension of the pathogen (either isolate Ahco2 or Noco2) and shifted to SD conditions. Thirty hr postinoculation (hpi), the interaction sites were classified as follows: (A), haustorium; (B), haustorium with plant cell reaction; (C), HR; (D), free hyphae; (E), hyphae with plant cell reaction; and (F), HR with emerging hyphae. h, haustorium; hy, hyphae; HR, hypersensitive response; pcr, plant cell reaction; s, spore. See text for details. Bar, 20 μm.

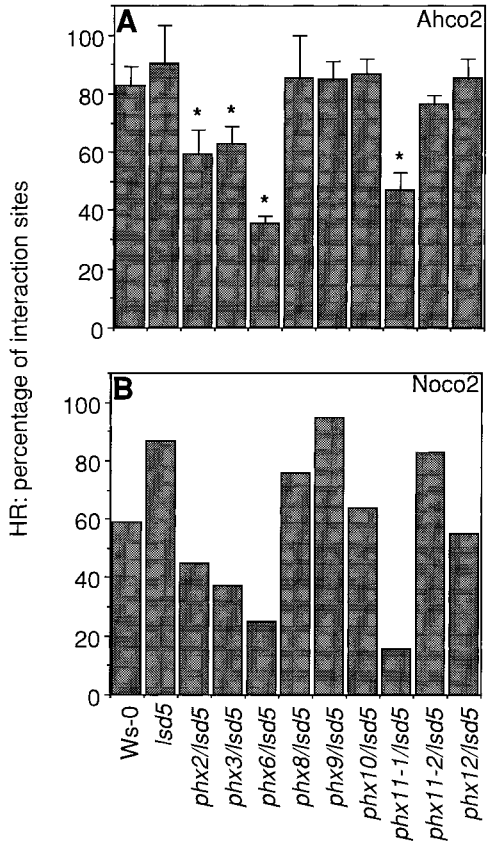

Figure 5.—Differential modification of the HR mediated by separate *R*-genes in the *phx*/*lsd5* mutants in response to *P. parasitica* isolates Ahco2 and Noco2. Two-week-old seedlings were spray-inoculated with a spore suspension of either isolate of *P. parasitica*. Tissues were stained using trypan blue as a marker of cell death 1 dpi, and the percentage of HR was determined (reaction types as defined in Figure 4C). (A) Isolate Ahco2; each point represents the mean and standard deviation of three to four independent experiments of 25–150 interaction sites on 5–30 cotyledons. Star denotes that a statistically significant difference was found using a *t*-test (95% confidence limit) between the *phx*/*lsd5* line and Ws-0 or *lsd5*. (B) Isolate Noco2. One representative experiment from three experiments. All experiments were scored blind.

both isolates, the suppressor lines *phx2*/*lsd5*, *phx3*/*lsd5*, *phx6*/*lsd5*, and *phx11-1*/*lsd5* displayed significantly fewer HR sites than either Ws-0 or *lsd5* (Figure 5). The other suppressor lines were not significantly different from *lsd5*. Interestingly, the *phx11-2* allele did not exhibit reduced HR as observed with the *phx11-1* allele. This suggests that despite the absence of visible *lsd5* lesions in growth conditions used in these experiments, the presence of *lsd5* in the background renders weak suppressors (*e.g.*, *phx11-2*; see Figure 1) slightly more resistant compared to Ws-0 (see also below). Little or no further growth of the pathogen was visible 5 dpi in Ws-0 and *lsd5*. However, in some of the lines where a reduced number of HRs was observed 1 dpi, hyphal growth had occurred 5 dpi, along with extensive cell death (data not shown and see below). We never observed asexual sporulation in any of the suppressor lines or Ws-0 and *lsd5* controls.

We then tested whether any of the suppressor mutations modified susceptibility to a normally virulent isolate of *P. parasitica*. Plants grown under LD were inoculated with the virulent isolate Emwa1 and shifted to SD. The putative intragenic suppressor mutant *phx2*/*lsd5* exhibited enhanced susceptibility to the pathogen, as demonstrated by a threefold increase in sporulation in this line as compared to *lsd5* (Figure 6). The other *phx*/*lsd5* lines showed sporulation levels similar to those in *lsd5* or Ws-0. *lsd5* mutants were as susceptible as wild-type Ws-0, confirming that the conditions used in these experiments do not significantly trigger *lsd5*-mediated resistance as observed under SD (Dietrich *et al.* 1994).

The *phx* mutations define previously unidentified loci:

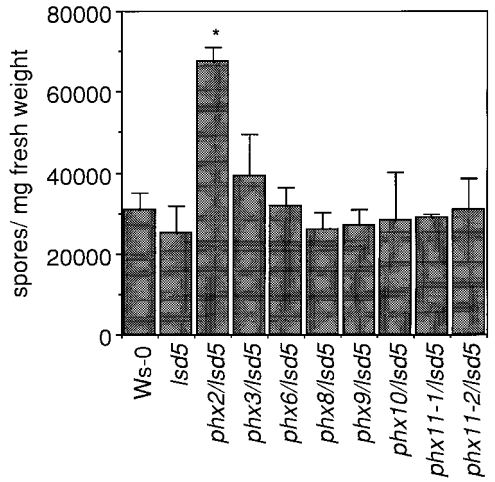

Figure 6.—Growth of the compatible *P. parasitica* isolate Emwa1 in the *phx*/*lsd5* lines. Two-week-old seedlings grown under LD were sprayed with a spore suspension of the pathogen and shifted to SD conditions. Sporulation was quantified 1 wk after inoculation. The data represent the mean and standard deviation from two independent experiments. Star denotes that a statistically significant difference was found using a *t*-test (95% confidence limit) between the *phx2*/*lsd5* line and Ws-0 or *lsd5*. All experiments were scored blind.

From the experiments described above, it appeared that several of the *phx*/*lsd5* mutants affected resistance determined by multiple *R*-genes. Several recessive mutations required for *R*-gene function (collectively termed *RDR*, required for disease resistance; Hammond-Kosack and Jones 1996) have been identified in Arabidopsis, and different screening procedures have sometimes led to the identification of mutations at the same locus (*e.g.*, Glazebrook *et al.* 1996). Therefore, some *phx* mutations could be allelic to known *RDR* mutations. Allelism between the *phx* mutations and three well-characterized *RDR* mutants, *ndr1-1* (Century *et al.* 1995, 1997), *pad4-1* (Glazebrook *et al.* 1997), and *eds1-1* (Parker *et al.* 1996), was examined.

For the *phx2*, *phx11-1*, *phx11-2*, and *phx3* mutants, allelism was ruled out by mapping. In the case of *phx2*, *phx11-1*, and *phx11-2* mutants, strong genetic linkage was found with the *lsd5* locus (Table 1). The *lsd5* mutant (Ws-0 background) was crossed to the polymorphic wild-type ecotypes La-er or Col-0. *lsd5* phenotype F_2 plants were used for mapping using CAPS and SSLP PCR markers (Konieczny and Ausubel 1993; Bell and Ecker 1994). Linkage to *lsd5* was found on the bottom of chromosome *2*, 1.2 cM telomeric to AthBIO2. As none of *ndr1-1*, *pad4-1*, or *eds1-1* maps to chromosome *2* (Holub 1997 and references therein), we concluded that *phx2*, *phx11-1*, and *phx11-2* are not allelic to them. The dominant *phx3* mutation was mapped via the wild-type *PHX3* recessive allele. The double mutant *phx3*/*lsd5* was crossed to Col-0, and F_2 plants that showed *lsd5* lesions (double homozygote *lsd5*/*PHX3*) were used for mapping. Linkage to chromosome *5* was found between markers nga76 and spl2. As expected, linkage to chromosome *2* corresponding to the *lsd5* locus (for which the mapping population was selected) was also found.

The recessive *phx*/*lsd5* mutants were each crossed to *ndr1-1*, *pad4-1*, and *eds1-1* recessive mutants. For complementation in the F_1 progenies, in which the recessive *lsd5* mutation has no impact, we tested for recovery of phenotypes associated with the test *RDR*-type mutations (see materials and methods). None of the tested *phx*/*lsd5* lines were allelic to any of these *RDR* mutations in F_1 plants, and recovery of *lsd5* lesions in the F_2 progeny further confirmed this conclusion (not shown). These results are consistent with the fact that *lsd5* lesions are not suppressed in *eds1-1*/*lsd5* or *ndr1-1*/*lsd5* double mutants (data not shown). We conclude that the *phx* mutants define new loci that can differentially modify *R*-gene function.

Genetic separation of the *phx* mutations from the *lsd5* mutation: Because the *lsd5* mutation confers heightened levels of disease resistance under SD (Dietrich *et al.* 1994), there was a possibility that the phenotypes observed in the *phx*/*lsd5* lines were combinatorial. Therefore, it was critical to isolate the *phx* mutations from the *lsd5* mutation. Because the *phx2*, *phx8*, *phx11-1*, and *phx11-2* mutations are linked to *lsd5* (and potentially intragenic; Table 1), we did not attempt to separate them from the *lsd5* mutation. Lines carrying four suppressor mutations (*phx3*, *phx6*, *phx9*, and *phx12*) exhibiting various degrees of suppression (Figure 1) were isolated.

The principle of isolation of the *phx* mutations is described in materials and methods. A PCR marker that is linked to the *lsd5* mutation was used to assist the isolation of the *phx* mutations, on the assumption that this marker was reliably reflecting the *lsd5* genotype (see materials and methods). Putative isolated *phx* lines were then backcrossed to *lsd5* and Ws-0 to check for the absence of the *lsd5* mutation and for homozygosity at the *phx* locus. For *phx3*, progeny from 18 independent (Ws-0 × *phx3*) F_2 backcross families segregated no *lsd5* plants, proving that the *phx3* line was homozygous *LSD5*. This was confirmed in that all nine independent F_2 progenies from the *phx3* × *lsd5* cross segregated 15 wild type: 1*lsd5*, indicating that the line isolated was homozygous for the *phx3* mutation and that this mutation was extragenic and dominant. Similar analysis was done with the recessive *phx6*, *phx9*, and *phx12* mutations (data not shown). None of the isolated *phx* lines showed any visible phenotype.

Bacterial resistance in the *phx3* and *phx6* mutants: We first assessed bacterial growth in *phx3* and *phx6* using *Pst* DC3000 (with or without *avrRpm1*). As shown in Figure 7A, the *phx3* line allowed significantly more growth of the normally avirulent *Pst* DC3000 (*avrRpm1*) than Ws-0. In addition, disease symptoms were visible in *phx3* 3 dpi (Figure 3A). We conclude from this experiment that the observed reduced disease resistance in

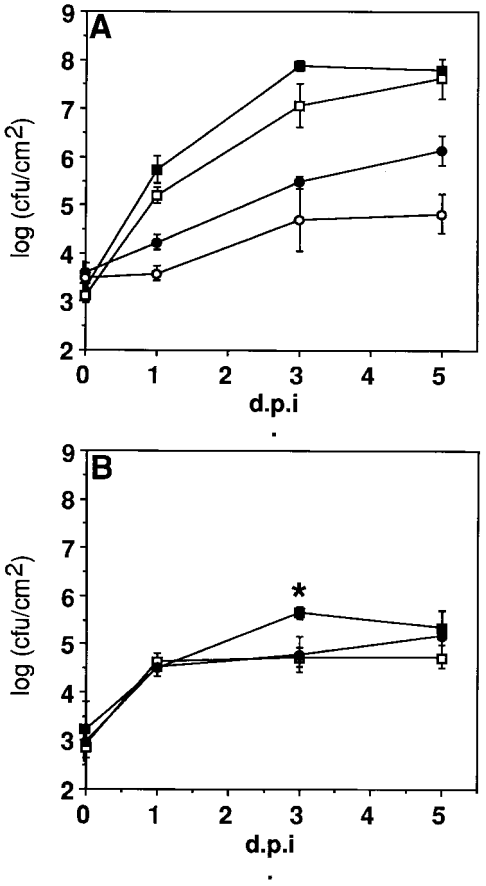

Figure 7.—Bacterial growth in the *phx3* and *phx6* single mutants. Plants grown under SD were hand-inoculated with 10^5 cfu/ml of *Pst* DC3000 (+/− *avrRpm1* or *avrRps4*). At the indicated times, samples were cut from infected leaves, and bacterial titers were determined. Each point represents the mean and standard deviation of three to four independent experiments. (A) Bacterial growth in the *phx3* mutant. Squares, *Pst* DC3000; circles, *Pst* DC3000 (*avrRpm1*). Open symbols, Ws-0; solid symbols, *phx3*. The *t* values and confidence limit for *Pst* DC3000 (*avrRpm1*) between *phx3* and *Ws-0* are 4.5 (>99%, 1 dpi) and 3.88 (>98%, 5 dpi). (B) Growth of *Pst* D3000 (*avrRps4*) in *phx3* (solid squares), *phx6* (solid circles), and Ws-0 (open squares). The star denotes a significant difference between *phx3* and Ws-0 (*t*-test value 5.65, >99%).

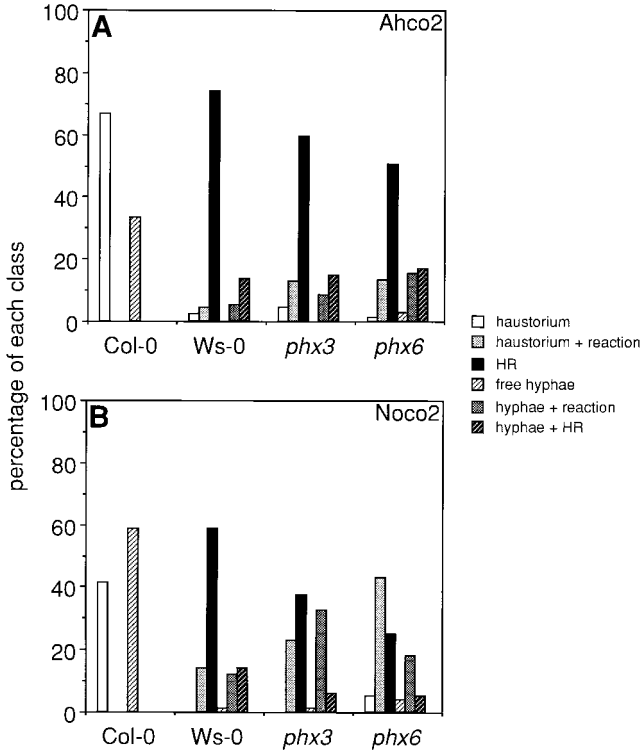

Figure 8.—Incompatible isolates of *P. parasitica* in the *phx3* and *phx6* mutants. Two-week-old seedlings were spray-inoculated with a spore suspension of the different isolates of *P. parasitica*. Tissues were stained using trypan blue as a marker of cell death 30 hpi, and the percentage of each class of reaction was determined (see text for details). Similar results were obtained in independent experiments, and one representative experiment is shown for each isolate. All experiments were scored blind. (A) Isolate Ahco2. Twenty cotyledons examined (representing 100–130 interaction sites) per genotype. (B) Isolate Noco2. Twenty cotyledons examined (representing 80–100 interaction sites) per genotype.

the *phx3/lsd5* line is caused by the *phx3* mutation itself. When challenged with the virulent *Pst* DC3000, the *phx3* lines showed enhanced susceptibility compared to Ws-0 (Figure 7A) and this was also correlated with increased chlorosis (Figure 3B). This enhanced susceptibility could be reverted by application of benzothiadiazole (125 mg/ml, not shown), an inducer of SAR (Görlach *et al.* 1996). When inoculated with the normally avirulent *Pst* DC3000 (*avrRps4*), *phx3*, but not *phx6*, showed slightly reduced resistance compared with Ws-0 (Figure 7B). This was not accompanied by appearance of symptoms as observed with the interaction between *phx3* and *Pst* DC3000 (*avrRpm1*). This suggests that *phx3* alters resistance triggered by *RPM1* more than resistance triggered by *RPS4*. In contrast, no significant difference was detected in the *phx6*, *phx9*, and *phx12* lines with either *Pst* DC3000 or *Pst* DC3000 (*avrRpm1*, not shown).

We also used a bacterial isolate of *P. syringae* pv. *glycinea*, which is nonpathogenic on Arabidopsis, to assess delivery of avirulence to the *phx* mutants. Typical necrosis was visible 7 hr after inoculation with *Psg* (*avrRpm1*) in the *phx3*, *phx6*, *phx9*, and *phx12* mutants (not shown). Thus we concluded that HR following high-dose inoculation is not impaired in these mutants.

Peronospora resistance in the *phx* mutants: The isolated *phx* mutants were also tested for their reaction to both incompatible and compatible isolates of *P. parasitica*. In contrast to simply measuring changes in HR frequency, as shown in Figure 5 for *phx/lsd5* lines, we performed detailed histology experiments, as defined in Figure 4.

When challenged with the incompatible isolates Ahco2 and Noco2, we observed a reduction in the number of HR present 1 dpi in both *phx3* and *phx6* (Figure 8), similar to our observations with the corresponding *phx/lsd5* lines (Figure 5). Therefore, the *phx3* and *phx6*

mutations are responsible for the reduced resistance previously detected. The reduction of the number of HRs in reaction to Ahco2 (Figure 8A) was not as pronounced as the one observed in the case of Noco2 (Figure 8B), and this parallels the results obtained with these isolates when tested on the *phx*/*lsd5* lines (Figure 5). In the case of Noco2, the increase in interaction sites containing haustoria, or hyphae, accompanied by plant cell reaction was more striking than that in Ws-0. This suggests that *R*-gene action is delayed in *phx3* and *phx6*, as these types of reactions precede the development of HR (Figure 4). Five dpi, the Peronospora life cycle was complete in Col-0, as demonstrated by profuse hyphal growth (Figure 9A) and oosporangia production. The resistant ecotype Ws-0 supported little hyphal growth and most of the reactions observed were complete HRs (Figure 9B). As a consequence of delayed triggering of the HR, pathogen growth occurred in *phx3* (Figure 9C), followed by development of massive cell death along hyphal tracks. We did not observe further growth of the pathogen in *phx6*, suggesting that this mutant was only affected in early stages of the interaction with *P. parasitica* (Figure 9D). However, neither pathogen isolate completed its life cycle as measured by lack of sporulation. The *phx9* and *phx12* lines did not show any significant difference from Ws-0 when challenged with isolate Ahco2 or Noco2 (not shown). Also, we did not observe modified susceptibility of the *phx* lines isolated when challenged with the virulent isolate Emwa1 (not shown), consistent with results presented in Figure 6.

DISCUSSION

We devised a screening procedure to genetically decipher the pathway(s) regulating cell death in Arabidopsis. This screening was also designed to address the role of a single component, cell death, in the multifaceted HR phenomenon. Our screening did not rely on phenotypes such as loss of resistance, as in the case of the screenings used to identify the *ndr1* (Century *et al.* 1995) or *eds* (Glazebrook *et al.* 1996; Parker *et al.* 1996) mutants. We used the spontaneous cell death phenotype of the *lsd5* mutant as a way to isolate suppressors of cell death and then assayed the effects of such mutations on disease resistance. In a similar manner, Glazebrook and Ausubel (1994) and Glazebrook *et al.* (1997) addressed the role of camalexin in resistance with the phytoalexin-deficient (*pad*) mutants. Our screening led to the identification of 10 *phx* genes, as determined by allelism tests, and our screen is obviously not saturating for this phenotype.

It has been proposed that *lsd* mutations represent defects in genes regulating the HR. Recessive mutations such as *lsd5* may be a loss-of-function of a gene normally negatively regulating the HR (Dangl *et al.* 1996; Mittler and Lam 1996). It was also suggested that some *lsd* mutations could lead to metabolic perturbations that would result in cell death (Dangl *et al.* 1996). We found that several suppressors of the *lsd5* cell death modify disease resistance response. This result confirms that the *lsd5* mutation results in upregulation of a disease resistance pathway. Moreover, this finding validates the use of *lsd* mutants to study the disease resistance pathway. The amenability of the lethal screening used to recover the *phx* mutants could allow for an extensive analysis of the disease resistance pathway.

In plants, cell death is involved in many aspects of normal development such as xylogenesis, reproduction, and senescence (Jones and Dangl 1996; Greenberg 1996). We did not observe any obvious morphological modification in the *phx*/*lsd5* and *phx* lines. This suggests

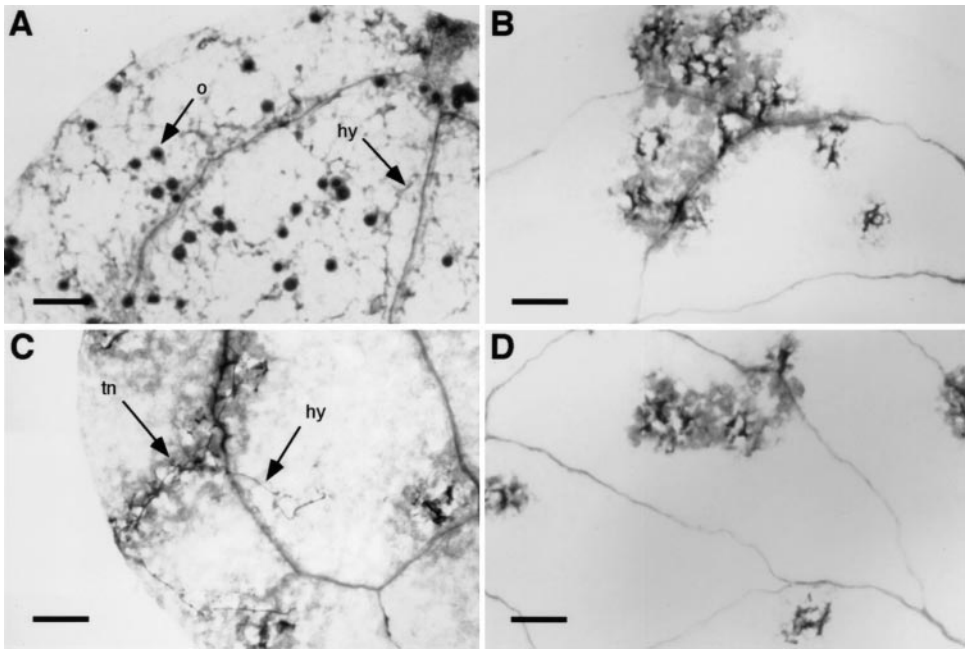

Figure 9.—Trailing necrosis in the *phx3* mutant. Plants were inoculated with *P. parasitica* Ahco2 as in Figure 8 and tissue was stained 5 dpi for microscopical examination. (A) Col-0, absence of cell death, profuse hyphal growth and elaboration of oosporangia. (B) Ws-0, HR, and no hyphal growth. (C) *phx3*, HR accompanied by free hyphal growth that eventually triggers trailing necrosis. (D) *phx6*, HR and no hyphal growth. hy, hyphae; o, oosporangia; tn, trailing necrosis. Bar, 20 μm.

that programs specific to each developmental process regulate cell death and that the *phx* mutations described here may be specific to disease resistance.

A range of suppressed phenotypes was found. We found no uncoupling of cell death suppression and suppression of *PR1* expression. Instead, there was a correlation between the extent of residual *lsd5*-dependent cell death and *PR1* expression (Figure 1). Genetic analysis of the disease resistance pathway led to several models in which cell death was placed upstream of SA-dependent defense gene activation (Dangl *et al.* 1996; Ryals *et al.* 1996). For example, the dominant *lsd2* and *lsd4* mutants (Hunt *et al.* 1997) and the recessive *cpr5* mutant (Bowling *et al.* 1997) still showed spontaneous lesions when crossed to *nahG* transgenic plants that accumulate very low levels of SA. In contrast, SA-dependent gene induction was suppressed in these plants (Bowling *et al.* 1997; Hunt *et al.* 1997). These results showed that in the case of these mutations, suppressing defense gene expression (by removing SA) did not suppress the appearance of cell death. Thus, cell death can be upstream of the point of action of SA. Our results indicate that suppression of cell death also results in suppression of defense gene expression, suggesting that at least *lsd5* cell death acts upstream of defense gene activation. This suggests that the *phx* mutations may represent defects in common regulators of cell death and defense gene expression.

The strongest suppressor mutations (*phx2*, *phx3*, *phx6*, and *phx11-1*) significantly reduced resistance against several normally avirulent pathogens as compared with *lsd5* or Ws-0 (Figures 2 and 5). In these cases, suppression of the *lsd5* phenotype did not result in a simple reversion to a wild-type phenotype with respect to pathogen response. Furthermore, the slightly increased resistance of *lsd5* (Figure 5 and Dietrich *et al.* 1994) was converted to a decreased disease resistance in the *phx*/*lsd5* lines. This was also true when the *phx3* and *phx6* mutations were isolated from the *lsd5* mutation (Figures 7 and 8). Therefore, we concluded that the phenotypes observed were due to the *phx* mutations and not to their interaction with *lsd5*. Moreover, because isolation of the *phx* mutations from *lsd5* was based on the *lsd5* suppression phenotype, it is likely that the mutation suppressing *lsd5* lesions is the same as that impairing disease resistance. Supporting this hypothesis is the observation that the *phx2* and *phx3* mutations impair both *lsd5* lesion formation and disease resistance in a dominant manner (Figure 3A) and that the phenotypes described were observed in independent *phx3* and *phx6* isolation lines.

The *phx2* and *phx3* mutations affected resistance to both necrotrophic and biotrophic pathogens. This is similar to other known *RDR* mutants. For example, the *ndr1-1* and *pad4-1* mutants are impaired in their resistance to both necrotrophic bacteria and biotrophic pathogens (Century *et al.* 1995; Glazebrook *et al.* 1997). Altogether the existence of such mutants indicates possible convergence of the pathways controlling resistance to various types of pathogens. However, the *phx6* mutation showed impaired resistance to the isolates Ahco2 and Noco2 of the biotrophic oomycete *P. parasitica* (Figure 9B) but not to the different strains of *Pst* DC3000 tested (Figure 7B). This finding suggests a possible divergence of the pathways leading to resistance to necrotrophic and biotrophic pathogens. Alternatively, the signaling events triggered by *RPS4* may overcome the requirement for a fully functional *PHX6*, whereas the signals triggered by the *RPP1/10/14* complex require a fully functional *PHX6* for appropriate triggering of downstream events. Like other *RDR* mutations, such as the *pad* mutations (Glazebrook and Ausubel 1994; Glazebrook *et al.* 1997), the *phx* mutations show only partial loss of resistance and, although delayed, resistance was always the outcome of the interaction in the most affected *phx* lines. This probably reflects that the HR phenomenon is multifaceted and that modifying one element of the pathway cannot abolish it.

Mutational analyses of the disease resistance pathway have often led to the recovery of allelic mutations, independent of the mode of screening used. For example, in a screen for mutants showing enhanced disease susceptibility (*eds* mutants), Glazebrook *et al.* (1996) identified mutations in the *PAD2* and *NPR1* genes that had been recovered using different screening procedures (Cao *et al.* 1994). We asked if any of the *phx* mutations were allelic to the known *RDR* mutations *ndr1-1*, *pad4-1*, and *eds1-1* (Holub 1997 and references therein). Mapping and allelism tests showed that none of the tested *phx* mutations were allelic to these mutations. This was expected because neither the *ndr1-1* nor the *eds1-1* mutations suppress *lsd5* lesions.

As more *R*-genes are being cloned, at least two distinct classes have been established based on sequence similarities (Bent 1996). The first class (LZ-NBS-LRR class) is represented by genes showing a leucine-zipper (LZ), a nucleotide-binding site (NBS), and leucine-rich repeats (LRR). The genes from the second class (TIR-NBS-LRR) show similarities with the toll and interleukin-1 receptors (TIR) and also possess a NBS and LRRs. Recent reports suggest that these two classes reflect the existence of at least two different disease resistance signaling pathways. In this model (Aarts *et al.* 1998), one pathway, dependent on *NDR1*, would trigger resistance governed by genes of the LZ-NBS-LRR class, whereas another pathway, dependent on *EDS1*, would govern resistance triggered by genes of the TIR-NBS-LRR class. We analyzed disease resistance governed by *R*-genes from both classes in this study: *RPM1* belongs to the LZ-NBS-LRR class (Grant *et al.* 1995) while *RPS4* (B. Staskawicz, personal communication) and *RPP1/10/14* (Botella *et al.* 1998) belong to the TIR-NBS-LRR class. The *phx2* and *phx3* mutations modify resistance triggered by both subclasses of NBS-LRR genes. There-

fore, they must act downstream (or independently) of the pathways dependent on *NDR1* and *EDS1*.

All suppressor lines, and the *phx3* and *phx6* lines (not shown), retained the ability to express *PR1* after treatment with SA (Figure 1C). Therefore, these mutations must act upstream or independently of the point of action of SA. To our knowledge, the *phx2* and *phx3* mutations are the first mutations of this type described: They impair disease resistance downstream (or independently) of the *NDR1*- and *EDS1*-dependent pathways and before the point of action of SA. When tested, the *eds* mutants alter susceptibility to virulent pathogens but not resistance to avirulent ones (Rogers and Ausubel 1997). Other *eds* mutants have not been tested with both virulent and avirulent pathogens. However, the finding that some of the *eds* mutants represent mutations in the *NPR1* gene (Glazebrook *et al.* 1996) suggests that these mutations are likely to be found downstream of SA action. The *pad4-1* mutation is most likely to be similar to some of the *phx* mutations, because *pad4-1* mutants showed reduced resistance to both avirulent strains of *P. syringae* pv *maculicola* and avirulent isolates of *P. parasitica* (Glazebrook *et al.* 1997). In addition, SA can still induce defense gene expression in *pad4-1* mutants, suggesting that this mutation acts upstream of SA (Zhou *et al.* 1998).

Interestingly, *phx3* in isolation showed some level of enhanced susceptibility when challenged with *Pst* DC3000 (Figure 7A), and the *phx2*/*lsd5* double mutant exhibited enhanced susceptibility to the virulent isolate of *P. parasitica* Emwa1 (Figure 6) but no *eds* phenotype with *Pst* DC3000 (not shown). This suggests that the pathways leading to R-gene-mediated disease resistance share some components with basic resistance mechanisms that act to limit pathogen growth during compatible interactions. Similar observations have been made with the *eds1-1* and *pad4-1* mutants where both a decrease in resistance and an increase in susceptibility were measured (Parker *et al.* 1996; Glazebrook *et al.* 1997).

The lines *phx8*/*lsd5*, *phx9*/*lsd5*, *phx10*/*lsd5*, *phx11-2*/*lsd5*, and *phx12*/*lsd5* did not show any altered disease resistance to the different pathogens tested. Therefore, these suppressor mutations may not be in the disease resistance pathway. They may be affecting the initial perturbation caused by the *lsd5* mutation. For example, if the *lsd5* mutation leads to the accumulation of a toxic compound, subsequent cell death, and expression of defense-related markers, detoxification of this compound could revert the *lsd5* phenotype without affecting disease resistance. In addition, the *lsd5* mutation has been shown to more specifically affect the cells of the epidermis layer, and suppressors specific to this tissue are unlikely to alter disease resistance to pathogens developing in the mesophyl. However, it is possible that the presence of *lsd5* in these weak suppressor lines counterbalanced their weak effects on triggering resistance. Accordingly, we did not observe enhanced susceptibility to *Pst* DC3000 in the *phx3*/*lsd5* line while we did in the *phx3* mutant (Figure 7A). Likewise in the weakly suppressed *phx*/*lsd5* lines, it is possible that some residual resistance was effective due to the presence of the *lsd5* mutation in the background.

Whether in isolation or in the presence of the *lsd5* mutation, only the strongest suppressors showed altered disease resistance. This suggests that a certain suppression threshold must be reached in order to significantly perturbate disease resistance. We hypothesize that only the mutations strongly suppressing the *lsd5* phenotype have an impact on disease resistance. The comparison of the effects of the *phx11-1* and *phx11-2* alleles supports this hypothesis. While the strong *lsd5* suppressor allele *phx11-1*/*lsd5* shows impaired resistance to avirulent isolates of *P. parasitica*, the weak suppressor allele *phx11-2* does not (Figure 5). Accordingly, when isolated from the *lsd5* mutation, the weak suppressor mutations *phx9* and *phx12* still did not exhibit altered resistance to avirulent pathogens (not shown).

None of the *phx* suppressors abolished the HR cell death triggered by avirulent pathogens. In particular, biotrophic pathogens can still induce HR in the *phx* mutants. Because these pathogens do not primarily kill their host, but instead need living cells, it is unlikely that the cell death observed in the *phx* mutants is a result of the pathogen alone. Similarly, HR is retained in several *RDR* mutants (Glazebrook and Ausubel 1994; Century *et al.* 1995; Parker *et al.* 1996). Several models can explain the development of HR cell death in the presence of *lsd5* cell death suppressors. In the first, the overall amount of pathogen-triggered signals overcomes the suppression threshold of the *phx* mutations. This model supposes that the amount of *lsd5*-triggered signal is below the one generated by pathogen attack. Alternatively, several independent signaling pathways could trigger cell death during the HR and the *lsd5* suppressors could affect only one of them. Several signals are generated during the HR, such as reactive oxygen intermediates (Baker and Orlandi 1995) and ion flux changes (Atkinson and Baker 1989). Bifurcation of intracellular resistance responses has also been described. The *lsd5* suppressors may be able to block some of these signals but not others. In either model, the strength of the suppressor mutations is expected to influence the extent of alteration in disease resistance. Epistasis analysis between the *phx* mutants and other *lsd* mutants, as well as study of the physiological defects in these mutants, should allow refinement of models of disease resistance pathways.

We thank B. Staskawicz, J. Parker, and J. Glazebrook for sending seeds of *ndr1-1*, *eds1-1*, and *pad4-1* mutants, respectively. The *avrRps4* avirulence gene was also kindly provided by B. Staskawicz. We thank Robert A. Dietrich for his encouragement and valued discussions. J.-B. Morel was supported by a predoctoral fellowship from the French Ministry of Education and Research (MENESRIP), and this work is funded by National Institutes of Health grant 1R01GM5771-01 to J.D.

LITERATURE CITED

Aarts, N., M. Metz, E. Holub, B. J. Staskawicz, M. J. Daniels *et al.*, 1998 Different requirements for EDS1 and NDR1 by disease resistance genes define at least two R gene mediated signalling pathways in Arabidopsis. Proc. Natl. Acad. Sci. USA **95:** 10306–10311.

Agrios, G. N., 1988 *Plant Pathology*. Academic Press, London.

Atkinson, M. M., and C. J. Baker, 1989 Role of the plasmalemma H^+-ATPase in *Pseudomonas syringae*-induced K^+/H^+ exchange in suspension-cultured tobacco cells. Plant Physiol. **91:** 298–303.

Ausubel, F. M., R. Brent, R. E. Kingston, D. D. Moore, J. G. Seidman *et al.*, 1995 *Current Protocols in Molecular Biology*. Greene Publishing Associates / Wiley Interscience, New York.

Baker, C. J., and E. W. Orlandi, 1995 Active oxygen in plant pathogenesis. Annu. Rev. Phytopathol. **33:** 299–321.

Bell, C. J., and J. R. Ecker, 1994 Assignment of 30 microsatellite loci to the linkage map of Arabidopsis. Genomics **19:** 137–144.

Bent, A. F., 1996 Plant disease resistance genes: function meets structure. Plant Cell **8:** 1757–1771.

Bisgrove, S. R., M. T. Simonich, N. M. Smith, A. Sattler and R. W. Innes, 1994 A disease resistance gene in Arabidopsis with specificity for two different pathogen avirulence genes. Plant Cell **6:** 927–933.

Botella, M. A., J. E. Parker, L. N. Frost, P. D. Bittner-Eddy, J. L. Beynon *et al.*, 1998 Three genes of the Arabidopsis *RPP1* complex resistance locus recognize distinct *Peronospora parasitica* avirulence determinants. Plant Cell **10:** 1847–1860.

Bowling, S. A., J. D. Clarke, Y. Liu and X. Dong, 1997 The *cpr5* mutant of Arabidopsis expresses both NPR1-dependent and NPR1-independent resistance. Plant Cell **9:** 1573–1584.

Büschges, R., K. Hollricher, R. Panstruga, G. Simons, M. Wolter *et al.*, 1997 The barley *Mlo* gene: a novel trigger of plant pathogen resistance. Cell **88:** 695–705.

Cao, H., S. A. Bowling, A. S. Gordon and X. Dong, 1994 Characterization of an Arabidopsis mutant that is nonresponsive to inducers of systemic acquired resistance. Plant Cell **6:** 1583–1592.

Century, K. S., E. B. Holub and B. J. Staskawicz, 1995 *NDR1*, a locus of *Arabidopsis thaliana* that is required for disease resistance to both a bacterial and a fungal pathogen. Proc. Natl. Acad. Sci. USA **92:** 6597–6601.

Century, K. S., A. D. Shapiro, P. P. Repetti, D. Dahlbeck, E. B. Holub *et al.*, 1997 *NDR1*, a pathogen-induced component required for Arabidopsis disease resistance. Science **278:** 1963–1965.

Dangl, J. L., E. B. Holub, T. Debener, H. Lehnackers, C. Ritter *et al.*, 1992 Genetic definition of loci involved in Arabidopsis-pathogen interactions, pp. 393–418 in *Methods in Arabidopsis*, edited by C. Koncz, N.-H. Chua and J. Schell. World Scientific Publishing, Singapore.

Dangl, J. L., R. A. Dietrich and M. H. Richberg, 1996 Death don't have mercy: cell death programs in plant-microbe interactions. Plant Cell **8:** 1793–1807.

Debener, T., H. Lehnackers, M. Arnold and J. L. Dangl, 1991 Identification and molecular mapping of a single *Arabidopsis thaliana* locus determining resistance to a phytopathogenic *Pseudomonas syringae* isolate. Plant J. **1:** 289–302.

Dietrich, R. A., T. P. Delaney, S. J. Uknes, E. R. Ward, J. A. Ryals *et al.*, 1994 Arabidopsis mutants simulating disease resistance response. Cell **77:** 565–577.

Dietrich, R. A., M. H. Richberg, R. Schmidt, C. Dean and J. L. Dangl, 1997 A novel zinc-finger protein is encoded by the *Arabidopsis LSD1* gene and functions as a negative regulator of plant cell death. Cell **88:** 685–694.

Flor, H. H., 1947 Host-parasite interactions in flax rust: its genetics and other implications. Phytopathol. **45:** 680–685.

Glazebrook, J., and F. M. Ausubel, 1994 Isolation of phytoalexin-deficient mutants of *Arabidopsis thaliana* and characterization of their interactions with bacterial pathogens. Proc. Natl. Acad. Sci. USA **91:** 8955–8959.

Glazebrook, J., E. E. Rogers and F. M. Ausubel, 1996 Isolation of Arabidopsis mutants with enhanced disease susceptibility by direct screening. Genetics **143:** 973–982.

Glazebrook, J., M. Zook, F. Mert, I. Kagan, E. E. Rogers *et al.*, 1997 Phytoalexin-deficient mutants of Arabidopsis reveal that *PAD4* encodes a regulatory factor and that four *PAD* genes contribute to downy mildew resistance. Genetics **146:** 381–392.

Goodman, R. N., and A. J. Novacky, 1994 *The Hypersensitive Reaction in Plants to Pathogens: A Resistance Phenomenon*. APS Press, St. Paul.

Görlach, J., S. Volrath, G. Knauf-Beiter, G. Hengy, U. Beckhove *et al.*, 1996 Benzothiadiazole, a novel class of inducers of systemic acquired resistance, activates gene expression and disease resistance in wheat. Plant Cell **8:** 629–643.

Grant, M. R., L. Godiard, E. Straube, T. Ashfield, J. Lewald *et al.*, 1995 Structure of the Arabidopsis *RPM1* gene enabling dual specificity disease resistance. Science **269:** 843–846.

Gray, J., P. S. Close, S. S. Hantke, J. McElver, S. P. Briggs *et al.*, 1997 A novel suppressor of cell death in plants encoded by the *Lls1* gene of maize. Cell **89:** 25–31.

Greenberg, J. T., 1996 Programmed cell death: a way of life for plants. Proc. Natl. Acad. Sci. USA **93:** 12094–12097.

Greenberg, J. T., and F. M. Ausubel, 1993 Arabidopsis mutants compromised for the control of cellular damage during pathogenesis and aging. Plant J. **4:** 327–341.

Greenberg, J. T., A. Guo, D. F. Klessig and F. M. Ausubel, 1994 Programmed cell death in plants: a pathogen-triggered response activated coordinately with multiple defense functions. Cell **77:** 551–563.

Hammond-Kosack, K. E., and J. D. G. Jones, 1996 Resistance gene-dependent plant defense responses. Plant Cell **8:** 1773–1791.

Hinsch, M., and B. Staskawicz, 1996 Identification of a new Arabidopsis disease resistance locus, *RPS4*, and cloning of the corresponding avirulence gene, *avrRps4*, from *Pseudomonas syringae* pv *pisi*. Mol. Plant-Microbe Interact. **9:** 55–61.

Holub, E. B., 1997 Organization of resistance genes in Arabidopsis, pp. 5–26 in *The Gene-for-Gene Relationship in Plant-Parasite Interactions*, edited by I. R. Crute, E. B. Holub and J. J. Burdon. CAB International, New York.

Holub, E. B., and J. L. Beynon, 1997 Symbiology of mouse-ear cress and oomycetes. Adv. Bot. Res. **24:** 227–273.

Holub, E. B., J. L. Beynon and I. R. Crute, 1994 Phenotypic and genotypic characterization of interactions between isolates of *P. parasitica* and ecotypes of *Arabidopsis thaliana*. Mol. Plant-Microbe Interact. **7:** 223–239.

Hunt, M. D., T. P. Delaney, R. A. Dietrich, K. B. Weymann, J. L. Dangl *et al.*, 1997 Salicylate-independent lesion formation in Arabidopsis *lsd* mutants. Mol. Plant-Microbe Interact. **10:** 531–536.

Jones, A. M., and J. L. Dangl, 1996 Logjam at the Styx: programmed cell death in plants. Trends Plant Sci. **1:** 114–119.

Kobayashi, D. Y., S. J. Tamaki and N. T. Keen, 1989 Cloned avirulence genes from the tomato pathogen *Pseudomonas syringae* pv *tomato* confer cultivar specificity on soybean. Proc. Natl. Acad. Sci. USA **86:** 157–161.

Koch, E., and A. Slusarenko, 1990 Arabidopsis is susceptible to infection by downy mildew fungus. Plant Cell **2:** 437–455.

Konieczny, A., and F. M. Ausubel, 1993 A procedure for mapping Arabidopsis mutations using co-dominant ecotype-specific PCR-based markers. Plant J. **4:** 403–410.

Linthorst, H. J. M., 1991 Pathogenesis-related proteins in plants. Crit. Rev. Plant Sci. **10:** 123–150.

Mittler, R., and E. Lam, 1996 Sacrifice in the face of foes: pathogen-induced programmed cell death in plants. Trends Microbiol. **4:** 10–15.

Morel, J.-B., and J. L. Dangl, 1997 The hypersensitive response and the induction of cell death in plants. Cell Death Differ. **4:** 671–683.

Parker, J. E., E. B. Holub, L. N. Frost, A. Falk, N. D. Gunn *et al.*, 1996 Characterization of *eds1*, a mutation in Arabidopsis suppressing resistance to *Peronopora parasitica* specified by several different *RPP* genes. Plant Cell **8:** 2033–2046.

Parker, J. E., M. J. Coleman, V. Szabò, L. N. Frost, R. Schmidt *et al.*, 1997 The Arabidopsis downy mildew resistance gene *RPP5* shares similarity to the Toll and Interleukin-1 receptors with *N* and *L6*. Plant Cell **9:** 879–894.

Reignault, P., L. N. Frost, H. Richardson, M. J. Daniels, J. D. G. Jones *et al.*, 1996 Four Arabidopsis *RPP* loci controlling resistance to the Noco2 isolate of *Peronospora parasitica* map to regions known to contain other *RPP* recognition specificities. Mol. Plant-Microbe Interact. **9:** 464–473.

Rogers, E. E., and F. M. Ausubel, 1997 Arabidopsis enhanced dis-

ease susceptibility mutants exhibit enhanced susceptibility to several bacterial pathogens and alterations in *PR-1* gene expression. Plant Cell **9:** 305–316.

Ryals, J. A., U. H. Neuenschwander, M. G. Willis, A. Molina, H.-Y. Steiner *et al.*, 1996 Systemic acquired resistance. Plant Cell **8:** 1809–1819.

Smith, C. J., 1996 Accumulation of phytoalexins: defense mechanism and stimulus response system. New Phytol. **132:** 1–45.

Uknes, S., B. Mauch-Mani, M. Moyer, S. Potter, S. Williams *et al.*, 1992 Acquired resistance in Arabidopsis. Plant Cell **4:** 645–656.

Walbot, V., D. A. Hoisington and M. G. Neuffer, 1983 Disease lesion mimics in maize, pp. 431–442 in *Genetic Engineering of Plants*, edited by T. Kosuge and C. Meredith. Plenum Publishing Company, New York.

Ward, E. R., S. J. Uknes, S. C. Williams, S. S. Dincher, D. L. Wiederhold *et al.*, 1991 Coordinate gene activity in response to agents that induce systemic acquired resistance. Plant Cell **3:** 1085–1094.

Whalen, M. C., R. W. Innes, A. F. Bent and B. J. Staskawicz, 1991 Identification of *Pseudomonas syringae* pathogens of Arabidopsis and a bacterial locus determining avirulence on both Arabidopsis and soybean. Plant Cell **3:** 49–59.

Wolter, M., K. Hollricher, F. Salamini and P. Schulze-Lefert, 1993 The *mlo* resistance alleles to powdery mildew infection in barley trigger a developmentally controlled defence mimic phenotype. Mol. Gen. Genet. **239:** 122–128.

Yang, H., J. Mcleese, M. Weisbart, J.-L. Dionne and R. A. Aubin, 1993 Simplified high throughput protocol for Northern hybridization. Nucleic Acids Res. **21:** 3337–3338.

Zhou, N., T. L. Tootle, F. Tsui, D. F. Klessig and J. Glazebrook, 1998 *PAD4* functions upstream from salicylic acid to control defense responses in Arabidopsis. Plant Cell **6:** 1021–1030.

Communicating editor: V. Sundaresan